J. Fluid Mech. (2024), *vol*. 984, R8, doi:10.1017/jfm.2024.252

Chaos via type-II intermittency in a forced globally unstable jet

Zhijian Yang[1], Bo Yin[1], Yu Guan[2], Stephane Redonnet[1] and Larry K.B. Li[1],†

[1]Department of Mechanical and Aerospace Engineering, The Hong Kong University of Science and Technology, Clear Water Bay, Hong Kong

[2]Department of Aeronautical and Aviation Engineering, The Hong Kong Polytechnic University, Kowloon, Hong Kong

(Received 5 October 2023; revised 24 January 2024; accepted 1 March 2024)

We explore the transition to chaos in a prototypical hydrodynamic oscillator, namely a globally unstable low-density jet subjected to external time-periodic forcing. As the forcing strengthens at an off-resonant frequency, we find that the jet exhibits a sequence of nonlinear states: period-1 limit cycle → quasiperiodicity → intermittency → low-dimensional chaos. We show that the intermittency obeys type-II Pomeau–Manneville dynamics by analysing the first return map and the scaling properties of the quasiperiodic lifetimes between successive chaotic epochs. By providing experimental evidence of the type-II intermittency route to chaos in a globally unstable jet, this study reinforces the idea that strange attractors emerge via universal mechanisms in open self-excited flows, facilitating the development of instability control strategies based on chaos theory.

Key words: chaos, jets, nonlinear dynamical systems

1. Introduction

Open-jet flows are integral to a wide range of technological and natural processes. As such, their spatiotemporal stability and nonlinear dynamics have been widely studied (Huerre & Monkewitz 1990; Schmid & Henningson 2001). In the absence of counterflow, a jet whose density is similar to that of its surroundings is dominated by local convective instability, behaving as a spatial amplifier of extrinsic disturbances (Huerre & Monkewitz 1990). By contrast, a jet whose density is below a critical value can develop a large enough region of local absolute instability to become globally unstable, behaving as a self-excited oscillator with an intrinsic hydrodynamic mode (Chomaz, Huerre & Redekopp 1988;

† Email address for correspondence: larryli@ust.hk

Monkewitz *et al.* 1990; Hallberg & Strykowski 2006; Lesshafft & Marquet 2010; Coenen *et al.* 2017; Chakravarthy, Lesshafft & Huerre 2018; Nair, Deohans & Vinoth 2022). In nonlinear dynamics, this can be viewed as a transition from a fixed point to a limit cycle, which can occur via a supercritical or subcritical Hopf bifurcation (Zhu, Gupta & Li 2017; Lee *et al.* 2019; Zhu, Gupta & Li 2019). The self-excited flow oscillations arising from global instability can be destructive – especially when they interact constructively with acoustic, structural or other hydrodynamic modes – necessitating control action.

Previous studies have shown that time-periodic acoustic forcing is effective in controlling both the frequency and amplitude of the self-excited oscillations of a globally unstable jet (Sreenivasan, Raghu & Kyle 1989; Kyle & Sreenivasan 1993). Such control action can produce a range of synchronisation phenomena, including quasiperiodicity, phase trapping and locking, asynchronous and synchronous quenching, as well as saddle-node and inverse Neimark–Sacker bifurcations (Li & Juniper 2013*a*,*b*; Kushwaha *et al.* 2022). Surprisingly, however, the emergence of deterministic chaos – a fundamental concept in nonlinear dynamics – has yet to be established in a globally unstable jet, irrespective of the type of forcing.

Identifying the routes to chaos is key to gaining a better understanding of the universal mechanisms and symmetry-breaking processes that govern the transition from ordered to complex states, such as turbulence (Manneville 2010). It can also facilitate theoretical efforts to model, predict and control the behaviour of open self-excited flows (Huerre & Monkewitz 1990). In general, a nonlinear dynamical system can become chaotic via multiple universal routes (Ott 2002). Since the 1980s, three routes have received broad attention.

(i) Along the period-doubling route, varying a control parameter causes an existing periodic orbit to lose stability and be replaced by a new attracting periodic orbit of half the original frequency. This process repeats indefinitely, resulting in a period-doubling cascade that forms a self-similar structure in the bifurcation map (Feigenbaum 1978).

(ii) Along the Ruelle–Takens–Newhouse route, three Hopf bifurcations occur successively, yielding a quasiperiodic (torus, $\mathbb{T}^3$) attractor with three incommensurable frequencies. Such an attractor is unstable to even the smallest perturbations, transforming into a chaotic attractor by stretching and folding (Newhouse, Ruelle & Takens 1978).

(iii) Along the intermittency route, chaotic epochs emerge intermittently against a background of regular dynamics, even when the system parameters are fixed and free of substantial noise. Varying a control parameter causes the lifetime and frequency of the chaotic epochs to increase, eventually leading to a state of sustained chaos. In early studies of dissipative dynamical systems, Pomeau & Manneville (1980) discovered three possible types of intermittency leading to chaos: type I corresponding to a saddle-node bifurcation, type II corresponding to a subcritical Hopf bifurcation, and type III corresponding to an inverse period-doubling bifurcation. Many additional types, such as crisis-induced intermittency and on–off intermittency, have since been discovered (Ott 2002).

In fluid mechanics, all three of these classic routes to chaos have been observed, albeit mostly in closed flows (e.g. Rayleigh–Bénard convection; Gollub & Benson 1980) and in open-wake flows (Olinger & Sreenivasan 1988; Pasche, Avellan & Gallaire 2018). To date, only a few studies have reported definitive evidence of chaos in open-jet flows. Crucially, that evidence is largely limited to globally stable jets dominated by local

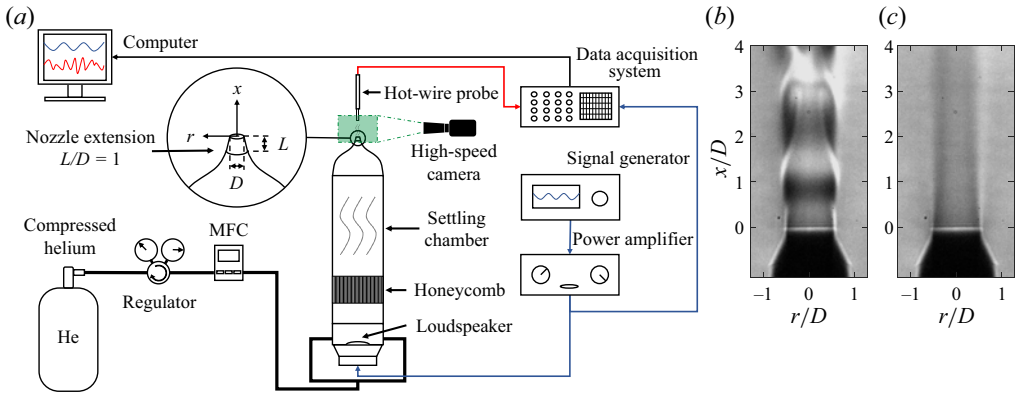

Figure 1. (*a*) Diagram of the experimental facility used to produce an axisymmetric jet of helium gas; MFC: mass flow controller. Also shown are schlieren snapshots of (*b*) a globally unstable jet at $Re = 648$ and (*c*) a globally stable jet at $Re = 385$, both for $S = 0.14$ and without external forcing. In the globally unstable jet (*b*), large-amplitude self-excited axisymmetric oscillations can be seen dominating the potential core.

convective instability. Such jets are exceptionally sensitive to extrinsic disturbances, making it challenging to distinguish between spatially amplified stochastic noise and low-dimensional deterministic chaos due to the flow itself (Huerre & Monkewitz 1990). Nevertheless, experimental and numerical evidence of chaos has been identified in globally stable equidensity jets subjected to external periodic forcing (Bonetti & Boon 1989) and to Reynolds number variations (Danaila, Dušek & Anselmet 1998). In both instances, the chaos was attributed to the collapse of helical flow structures in the near field of the jet. Moreover, Broze & Hussain (1996) observed a transition to low-dimensional chaos via type-II intermittency in a globally stable equidensity jet subjected to external periodic forcing. By contrast, the existence of chaos in a globally unstable jet, which hosts a natural hydrodynamically self-excited mode (Monkewitz *et al.* 1990; Hallberg & Strykowski 2006), has yet to be rigourously established. The sole evidence to date, from the seminal experiments of Sreenivasan *et al.* (1989), is merely suggestive, as it only hints at the possibility of chaos based on analogies between self-excited wakes and jets. Importantly, the routes to chaos in a globally unstable jet have yet to be identified.

In this experimental study, we report the first conclusive evidence of chaos in a globally unstable jet, and show that the chaos arises via type-II intermittency belonging to the class of Pomeau & Manneville (1980). By providing new insight into how strange attractors emerge in open self-excited flows, this study creates new opportunities for the development of instability control strategies based on chaos theory (Boccaletti *et al.* 2000). Below, we introduce our experimental set-up (§ 2), present evidence of the type-II intermittency route to chaos (§ 3), and conclude with the implications of this discovery (§ 4).

2. Experimental set-up

We generate a globally unstable jet by discharging gaseous helium into ambient air (296 K, 1 bar) using the same experimental facility that was used in our previous studies on the nonlinear dynamics of low-density jets (Zhu *et al.* 2017; Lee *et al.* 2019; Zhu *et al.* 2019). Shown in figure 1(*a*), the facility consists of a nozzle assembly, a helium supply system, and electronics for data acquisition and external forcing. The nozzle assembly contains a convergent section (area ratio of 100:1) with a round outlet of diameter $D = 6$ mm and extension length $L = D$. For an axisymmetric jet in the incompressible inertial regime, the onset of global instability is known to be determined by three primary parameters

(Hallberg & Strykowski 2006; Coenen *et al.* 2017; Chakravarthy *et al.* 2018; Nair *et al.* 2022): (i) the jet Reynolds number, $Re \equiv \rho_j U_j D/\mu_j$, where ρ_j and μ_j are the density and dynamic viscosity of the jet fluid, while U_j is the jet centreline velocity; (ii) the jet-to-ambient density ratio, $S \equiv \rho_j/\rho_\infty$, where ρ_∞ is the density of the ambient fluid; and (iii) the transverse curvature, D/θ_0, where θ_0 is the initial momentum thickness. In this study, we focus on a parameter combination ($Re = 648$, $S = 0.14$, $D/\theta_0 = 31.1$) just beyond the Hopf point, where an axisymmetric global mode exists at a natural frequency of $f_n = 497 \pm 5$ Hz. This frequency, which corresponds to a Strouhal number of $St = 0.23$ based on D and U_j, is within 15 % of the universal scaling proposed by Hallberg & Strykowski (2006) through considerations of a viscous time scale and the centripetal acceleration generated by the streamwise curvature of the oscillating jet column. Figure 1(*b*) shows a schlieren snapshot of this global mode, alongside an equivalent low-density jet without a global mode (figure 1*c*). In the former case, large-amplitude self-excited axisymmetric oscillations can be seen dominating the jet potential core.

To induce chaotisation, we subject the globally unstable jet to axisymmetric acoustic forcing generated by a loudspeaker mounted at the base of a cylindrical settling chamber containing a honeycomb flow straightener (see figure 1*a*). The loudspeaker is driven by a time-periodic signal with a normalised frequency of $f_f/f_n \in [1.75, 1.81]$ and a normalised amplitude of $\alpha \equiv A/A_c \in [0, 2.2]$, where f_f is the forcing frequency, A is the loudspeaker voltage and $A_c = 299\ \mathrm{mV_{rms}}$ is the critical voltage at the onset of intermittency. The significance of this specific range of forcing frequencies will be discussed later. At these forcing conditions, the root-mean-square velocity perturbations generated at the nozzle outlet are directly proportional to the loudspeaker voltage: $u'_{0,rms} = (2.8 \times 10^{-4}\ \mathrm{m\ s^{-1}\ mV^{-1}_{rms}})A$. We monitor the jet response with a constant-temperature single-wire anemometer (Dantec 55P16) located inside the jet potential core, specifically at $(x/D, r/D) = (1.5D, 0)$, where x and r are the streamwise and radial coordinates, respectively. At this sampling location, the jet dynamics is dictated by the wavemaker of the global mode, and the jet fluid (helium) concentration does not vary, enabling time traces of the local velocity $u(t)$ to be extracted from a precalibration. We use a 16-bit data acquisition system (NI USB-6212) to digitise the anemometer voltage at 65 536 Hz, which exceeds $100f_n$. We use a sampling duration of 8 s for most cases, but raise this to 60 s for cases showing any signs of intermittency in order to obtain converged statistics. For more information on the experimental set-up, please see our previous studies (Zhu *et al.* 2017; Lee *et al.* 2019; Zhu *et al.* 2019).

3. Results and discussion

3.1. *Intermittency route to chaos*

Li & Juniper (2013*a*,*b*) have shown that when a globally unstable jet is forced axially at an incommensurable frequency around $f_f/f_n = 1$, forced synchronisation can occur via two sequential transitions: (i) from a period-1 limit cycle to a $\mathbb{T}^2$ quasiperiodic attractor through a Neimark–Sacker bifurcation; and then (ii) from the $\mathbb{T}^2$ quasiperiodic attractor to a 1:1 synchronous orbit either through a saddle-node bifurcation, leading to phase locking, or through an inverse Neimark–Sacker bifurcation, leading to suppression.

In this study, we show that an alternative transition scenario can occur when f_f is within a specific range between the natural mode and its second harmonic, $f_f/f_n \in [1.75, 1.81]$. Figure 2 summarises this scenario for a representative case where $f_f/f_n = 1.78$. As the forcing amplitude α increases, the jet transitions through four dynamical states: limit

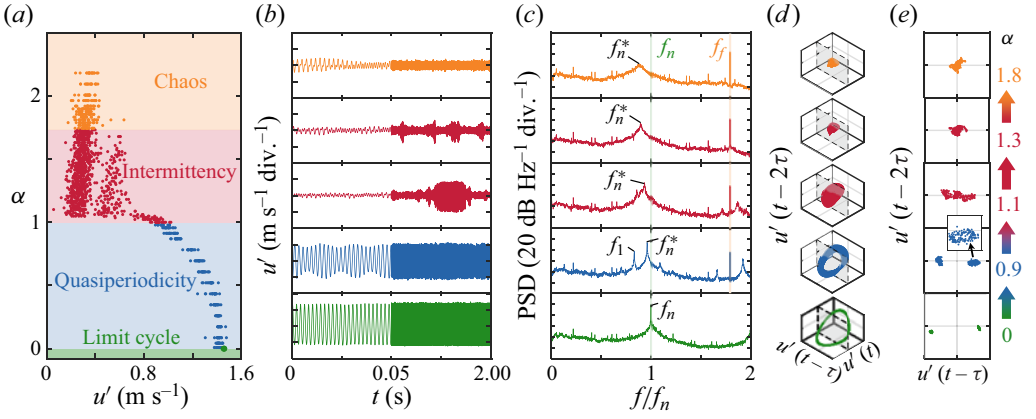

Figure 2. Overview of the type-II intermittency route to chaos in a forced globally unstable jet: (*a*) bifurcation map, (*b*) time traces of the velocity fluctuation u' with the window $t = 0$–0.05 s zoomed in, (*c*) PSD of u', (*d*) phase portraits, and (*e*) two-sided Poincaré maps. The forcing frequency is fixed at a representative value of $f_f/f_n = 1.78$, while the normalised forcing amplitude α is varied (see labels on the far right of (*e*)). Four dynamical states are highlighted: ($\alpha = 0$, green) period-1 limit cycle, ($\alpha = 0.9$, blue) $\mathbb{T}^2$ quasiperiodicity, ($\alpha = 1.1$ and 1.3, red) type-II intermittency and ($\alpha = 1.8$, orange) low-dimensional chaos. In panels (*d*,*e*), phase space reconstruction is performed via the embedding theorem of Takens (1981) with a delay time of $\tau = 0.52$ ms $\approx 1/(4f_n)$.

cycle → quasiperiodicity → intermittency → chaos. Next, we give an overview of these four states, before delving into a detailed analysis of the intermittent state in § 3.2.

(i) Limit cycle. When unforced ($\alpha = 0$), the jet oscillates in a period-1 limit cycle at the natural frequency of its global mode, f_n. This is evidenced by the tight concentration of data points in the bifurcation map (figure 2*a*), the regularity of the u' waveform (figure 2*b*), the sharp peak at f_n in the power spectral density (PSD; figure 2*c*), the closed orbit in the phase portrait (figure 2*d*), and the two clusters of intercepts in the two-sided Poincaré map (figure 2*e*). In figure 2(*d*,*e*), phase space reconstruction is performed via the embedding theorem of Takens (1981), with the optimal delay time ($\tau = 0.52$ ms) found via the first local minimum of the average mutual information function (Fraser & Swinney 1986). This delay time maximises the degree of attractor unfolding and corresponds to approximately one-quarter of the oscillation period of the natural global mode, $\tau \approx 1/(4f_n)$.

(ii) Quasiperiodicity. When forced at a low amplitude ($0 < \alpha < 1$), the jet continues to be globally unstable at f_n^*, where the superscript $*$ denotes the presence of forcing. However, the jet also responds at f_f, which is incommensurable with f_n^*, resulting in a transition to a two-frequency quasiperiodic state characterised by ergodic evolution on a two-dimensional torus attractor $\mathbb{T}^2$. This is indicated by the emergence of a toroidal structure in the phase portrait (figure 2*d*), giving rise to a pair of closed loops in the Poincaré map (figure 2*e*). It is also indicated by the amplitude modulations in the u' waveform (figure 2*b*) and by the coexistence of sharp peaks at both f_n^* and f_f in the PSD (figure 2*c*), along with a spectral component at the binaural modulation frequency, $f_1 = f_f - f_n^*$. These observations show that the jet has undergone a Neimark–Sacker bifurcation, transitioning from a period-1 limit cycle to a $\mathbb{T}^2$ quasiperiodic attractor when forcing is introduced.

(iii) Intermittency. When forced at a higher amplitude ($1 \leq \alpha < 1.74$), the jet remains quasiperiodic for some of the time, but becomes chaotic at other times. This intermittent switching is directly visible in the bifurcation map and the u' waveform (figure 2*a*,*b*),

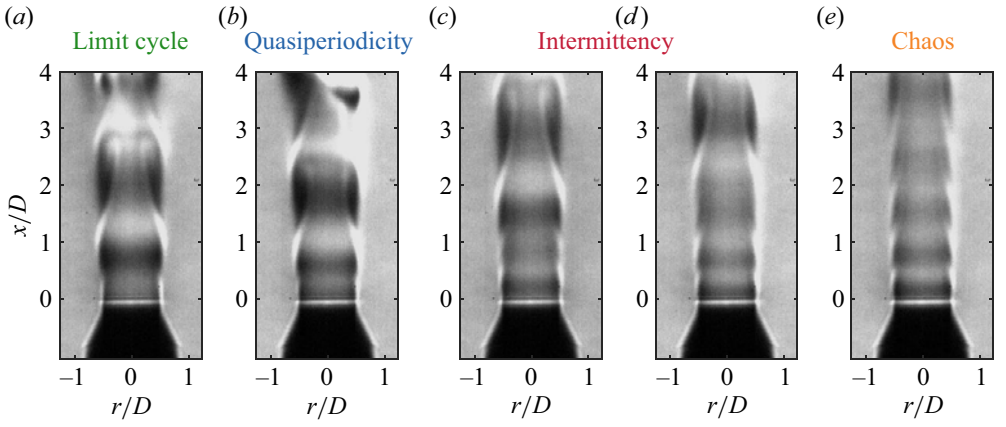

Figure 3. Schlieren snapshots of a globally unstable jet forced at the conditions of figure 2: (*a*) limit cycle at $\alpha = 0$, (*b*) quasiperiodicity at $\alpha = 0.9$, (*c*,*d*) intermittency at $\alpha = 1.1$ and 1.3 and (*e*) chaos at $\alpha = 1.8$.

where low-amplitude chaotic epochs appear intermittently amidst a background of mid-amplitude quasiperiodic dynamics. As α increases, both the lifetime and frequency of the chaotic epochs increase, ultimately yielding sustained chaos. Meanwhile, the PSD shows that the natural mode (f_n^*) is gradually pushed away from the forced mode (f_f), while its tonal nature becomes more broadband; this weakens the binaural effect that initially led to the apparent component at f_1 (figure 2*c*). The phase space contains a chaotic saddle at the core and a $\mathbb{T}^2$ orbit around its periphery (figure 2*d*,*e*). In § 3.2, we will examine the reinjection processes that govern how the jet switches between the two saddles.

(iv) Chaos. When forced at an even higher amplitude ($1.74 \leq \alpha \leq 2.2$), the jet ceases switching intermittently. Instead, it remains continuously on the chaotic attractor, taking on a low-amplitude state of sustained chaos. This is evidenced by the near-random scattering of data points in the bifurcation map (figure 2*a*), the irregularity of the u' waveform (figure 2*b*), the broadband spectral features of the PSD (figure 2*c*), and the intricate structures and trajectory intercepts in the phase space (figure 2*d*,*e*).

We use schlieren imaging to examine the spatial structure of the global mode, with a view to identifying the origin of the aperiodic dynamics. As figure 3 shows, the jet remains dominated by axisymmetric structures (zero azimuthal wavenumber) for all four dynamical states encountered in this study: limit cycle, quasiperiodicity, intermittency and chaos. The robustness of this axisymmetry suggests that the observed aperiodicity is not due to the excitation of helical modes.

Next, we apply three more tools from dynamical systems theory to verify the existence of chaos and characterise its fractal properties. For completeness, we also apply the same tools to the limit-cycle attractor ($\alpha = 0$) and the $\mathbb{T}^2$ quasiperiodic attractor ($\alpha = 0.9$).

First, we analyse the topological self-similarity of the attractors by estimating their active degrees of freedom. We do this through the correlation dimension ($\overline{D_c}$), as computed from the u' signal via the method of Grassberger & Procaccia (1983). We use 2^{16} data points in each computation and round the estimated $\overline{D_c}$ value to two significant figures, providing sufficient precision to distinguish between fractal and non-fractal behaviour. Figure 4(*ai*,*bi*,*ci*) shows the local gradient of the correlation sum ($D_c \equiv \partial \log C_N / \partial \log R$) vs the normalised hypersphere radius (R/R_{max}) for a delay time of $\tau = 0.52$ ms $\approx 1/(4f_n)$ and an embedding dimension of $m = 6$, 8 and 10. Here C_N is the correlation sum, R is the

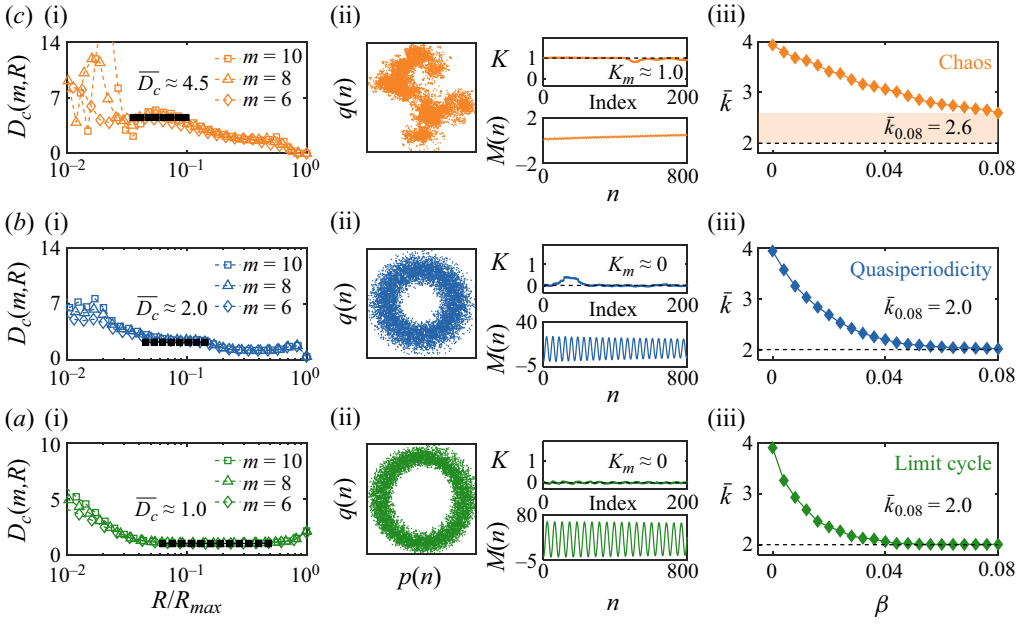

Figure 4. Evidence of low-dimensional chaos on a strange attractor: (*a*i–*c*i) the correlation-sum gradient vs the normalised hypersphere radius, (*a*ii–*c*ii) the translation components, mean squared displacement and asymptotic growth rate K from the 0–1 test, and (*a*iii–*c*iii) the mean degree of the filtered horizontal visibility graph vs the amplitude of the noise filter. The mean degree at a noise-filter amplitude of $\beta = 0.08$ is denoted as $\bar{k}_{0.08}$. Three dynamical states from figure 2 are shown: (*a*: green) period-1 limit cycle at $\alpha = 0$, (*b*: blue) $\mathbb{T}^2$ quasiperiodicity at $\alpha = 0.9$, and (*c*: orange) low-dimensional chaos at $\alpha = 1.8$.

hypersphere radius, and R_{max} is its maximum value. For the limit-cycle state (figure 4*a*i), D_c takes on a mean value of $\overline{D_c} \approx 1.0$ across the self-similar range of Euclidean scales ($0.06 \leq R/R_{max} \leq 0.5$), confirming that the jet evolves on a closed periodic orbit. For the quasiperiodic state (figure 4*b*i), $\overline{D_c} \approx 2.0$ across the primary self-similar range ($0.045 \leq R/R_{max} \leq 0.15$), which is consistent with a $\mathbb{T}^2$ torus attractor with two incommensurable modes. For the chaotic state (figure 4*c*i), $\overline{D_c}$ converges to a non-integer value of 4.5 across the self-similar range ($0.035 \leq R/R_{max} \leq 0.1$), indicating that this chaotic attractor is both strange and low-dimensional (Ott 2002).

Second, we confirm the presence of deterministic chaos by applying the 0–1 test of Gottwald & Melbourne (2004). For both the limit-cycle state (figure 4*a*ii) and the quasiperiodic state (figure 4*b*ii), the translation components $[p(n), q(n)$ with $n = 1, 2, \ldots, N]$ form a circular pattern, with the mean squared displacement $M(n)$ remaining bounded in time, resulting in a median growth rate of $K_m \approx 0$. These translation features indicate non-chaotic dynamics (Gottwald & Melbourne 2004). For the chaotic state (figure 4*c*ii), the translation components form a Brownian-like pattern, with $M(n)$ increasing linearly in time at a median rate of $K_m \approx 1$. These translation features indicate chaotic dynamics, which is consistent with the non-integer value of $\overline{D_c}$ found above and with our initial assessment of figure 2.

Third, we further confirm the presence of deterministic chaos by transforming the u' signal into complex networks using the filtered horizontal visibility graph of Nuñez *et al.* (2012). This tool can identify periodic structures concealed within noise-corrupted signals, allowing for the differentiation of chaotic, stochastic and noisy periodic dynamics. For both the limit-cycle state (figure 4*a*iii) and the quasiperiodic state (figure 4*b*iii), the mean

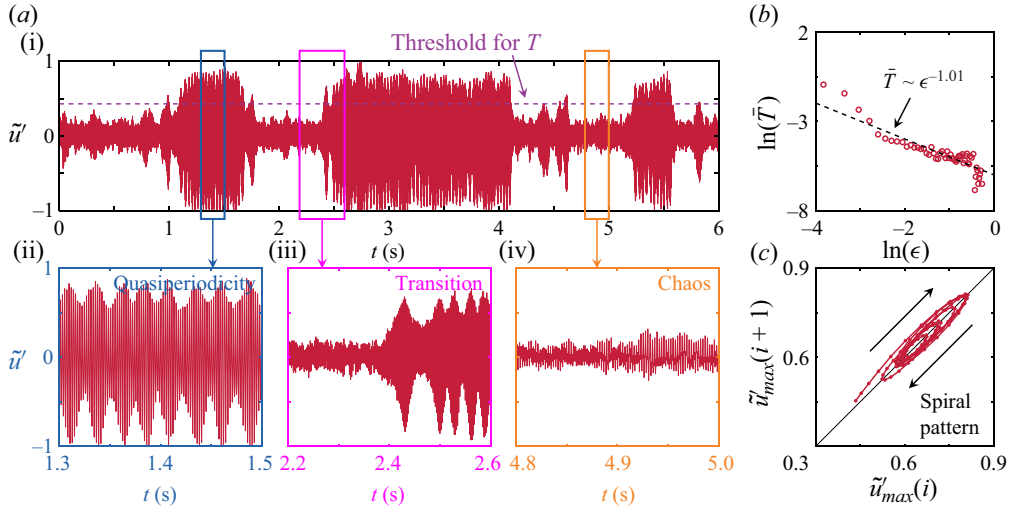

Figure 5. Evidence of type-II intermittency: (*a*) time traces of $\tilde{u}'$ showing irregular switching between quasiperiodicity and chaos, (*b*) the average inter-chaos time $\bar{T}$ vs the control parameter $\epsilon \equiv \alpha - 1$, and (*c*) the first return map of successive local maxima. In panels (*a*) and (*c*), the forcing amplitude is $\alpha = 1.1$ ($\epsilon = 0.1$).

degree $\bar{k}$ falls to exactly 2 as the amplitude of the graph–theoretical noise filter increases to a high value ($\beta = 0.08$). This indicates that both states are dominated by regular dynamics of temporal period $\mathcal{T} = 1$, which is consistent with the prevailing strength of the f_n mode in the limit-cycle case and that of the f_n^* mode in the quasiperiodic case (see the PSD in figure 2*c*). In the quasiperiodic case, there are also spectral components at f_f and f_1, but these are significantly weaker than the natural hydrodynamic mode at f_n^*, leaving the system to be dominated by the latter. For the chaotic state (figure 4*c*iii), $\bar{k}$ fails to converge even at a high value of β, indicating the absence of any periodic structure in the signal. When combined with the limited degrees of freedom ($\overline{D_c} \approx 4.5$), this confirms that this state is governed by chaotic processes, rather than by stochastic processes embedded in a periodic signal.

In summary, by applying the correlation dimension, the 0–1 test and the filtered horizontal visibility graph, we have found definitive evidence that a forced globally unstable jet can exhibit low-dimensional deterministic chaos on a strange attractor.

3.2. *Identification of the intermittency type*

We conduct a detailed analysis of the intermittent state ($1 \leq \alpha < 1.74$) to identify the route to chaos. Figure 5(*a*i) shows a partial segment of the full 60 s time series of the normalised velocity fluctuation, $\tilde{u}'(t) \equiv u'(t)/u'_{max}$, where u'_{max} is the maximum velocity fluctuation. We observe intermittent switching between mid-amplitude quasiperiodic epochs (figure 5*a*ii) and low-amplitude chaotic epochs (figure 5*a*iv) via a transition regime (figure 5*a*iii). We use two methods to identify the intermittency type.

First, we compile statistics on the lifetime (T) of every quasiperiodic epoch (i.e. the regular phase) using a velocity amplitude threshold of $\tilde{u}' = 0.43$, as indicated by the horizontal dashed line in figure 5(*a*i); T is also known as the inter-chaos time. We use this threshold value as it provides a robust balance between rejecting the chaotic epochs and capturing the quasiperiodic epochs. A sensitivity analysis of the scaling properties of T reveals no significant variation within a threshold range of $\tilde{u}' \in [0.40, 0.45]$. Figure 5(*b*)

shows on double-logarithmic axes the average value of T, or $\bar{T}$, as a function of the proximity to the critical forcing amplitude at the onset of intermittency, $\epsilon \equiv \alpha - 1$. We find that $\bar{T}$ decreases as ϵ increases, indicating that the quasiperiodic dynamics is gradually replaced by chaotic dynamics as the forcing strengthens. The gradual nature of this replacement process is characteristic of the intermittency route to chaos (Ott 2002; Schuster & Just 2005). Crucially, we find an inverse power-law relationship of the form $\bar{T} \sim \epsilon^{-1.01}$, where the exponent has a 95 % confidence limit of ± 0.15. According to the reinjection theory of Pomeau & Manneville (1980), the power-law exponent is expected to be -1 for type-II or type-III intermittency, but $-1/2$ for type-I intermittency. Therefore, the power-law exponent of -1.01 observed in figure 5(*b*) rules out the possibility of type-I intermittency in our system.

Second, we plot in figure 5(*c*) an array of successive local maxima $\tilde{u}'_{max}(i)$ extracted from the regular phase (quasiperiodicity) along with a copy of itself shifted by one sample index $\tilde{u}'_{max}(i+1)$. This is known as the first return map, whose features can reveal the intermittency type (Ott 2002). Previous studies have established that the data points in the first return map pass through a tunnel next to the main diagonal for type-I intermittency (Schuster & Just 2005), they form a spiral pattern for type-II intermittency (Arneodo, Coullet & Tresser 1981; Sacher, Elsässer & Göbel 1989; Ganapathy & Sood 2006), and they cross the main diagonal along a tangent-function-like path for type-III intermittency (Griffith *et al.* 1997). In figure 5(*c*), the data points form a clear spiral pattern, confirming that the intermittency in our system is of type II.

In summary, by analysing the scaling behaviour of the average inter-chaos time and the first return map, we have determined that the intermittency observed en route to chaos in our jet conforms to type II of the Pomeau & Manneville (1980) classification.

4. Conclusions and discussion

Previous reports of chaos in open-jet flows have been limited to globally stable jets dominated by local convective instability. In this experimental study, we have provided the first conclusive evidence of chaos in a globally unstable jet: an axisymmetric inertial low-density jet containing a large enough region of local absolute instability to support a hydrodynamically self-excited global mode. We found that when forced externally with an increasing amplitude at an off-resonant frequency ($f_f/f_n \in [1.75, 1.81]$), the jet exhibits a sequence of nonlinear states: period-1 limit cycle $\rightarrow$ quasiperiodicity on a $\mathbb{T}^2$ torus attractor $\rightarrow$ type-II intermittency of the Pomeau & Manneville (1980) class $\rightarrow$ low-dimensional chaos on a strange attractor. We verified the low-dimensional fractal nature of the chaotic state through (i) the correlation dimension converging to a non-integer value of $\overline{D_c} \approx 4.5$, (ii) the 0–1 test returning Brownian-like translation patterns and a growth rate of the mean squared displacement of $K_m \approx 1$, and (iii) the filtered horizontal visibility graph exhibiting a non-converging mean degree. The intermittent state features switching between mid-amplitude quasiperiodic epochs and low-amplitude chaotic epochs. We verified the type-II nature of this state through (i) the power-law relationship between the average inter-chaos time $\bar{T}$ and the control parameter ϵ, with a scaling exponent approaching the theoretical value of -1, and (ii) the first return map showing a clear spiral pattern. When considered together, these observations offer compelling evidence that the globally unstable jet has transitioned into a state of low-dimensional chaos on a strange attractor via type-II intermittency conforming to the class of Pomeau & Manneville (1980).

The discovery of the type-II intermittency route to chaos in a forced globally unstable jet has several implications. First, it strengthens the argument that strange attractors

emerge via universal mechanisms in open self-excited flows (Huerre & Monkewitz 1990; Manneville 2010). This could accelerate the development of instability control strategies for such flows by leveraging both emerging and established actuation concepts from chaos theory (Boccaletti *et al.* 2000). Second, the type-II intermittency route to chaos has also been observed in various other dynamical systems in nature and engineering, and can be readily modelled (Ott 2002; Schuster & Just 2005). This suggests that it might be possible to build on those existing modelling efforts to better understand and predict the stability and dynamics of open self-excited flows, especially their transition from a regular state to a chaotic state en route to turbulence. Third, the presence of chaos in an open self-excited flow can be detrimental in situations where the flow interacts with a deformable structure or an acoustic field. This is because such chaotic flow oscillations would generate broadband spectral components with the potential to readily excite resonant modes in the structure or acoustic field. Encouragingly, the presence of intermittency preceding chaos in the present flow suggests that it might be possible to detect precursors of chaos using proven tools such as complex networks, multifractal analysis, and recurrence quantification analysis (Sujith & Unni 2020). Fourth, our findings reveal that even when subjected to strong periodic forcing, a globally unstable jet may not necessarily synchronise with that forcing. Instead, it can exhibit far more complex dynamics, such as intermittency and strange chaotic attractors. In the field of nonlinear dynamics, the breakdown of a $\mathbb{T}^2$ torus into chaos due to strong external forcing has been analysed by Aronson *et al.* (1982) using a family of maps, with Afraimovich & Shilnikov (1991) focusing on the specific case of a phase-locked torus. Intermittency can occur in two of the main breakdown scenarios, one involving the birth of a homoclinic orbit and the other involving the formation of a non-smooth manifold homeomorphic to the torus (Pikovsky, Rosenblum & Kurths 2003). Both scenarios are found only near the outer regions of the Arnold tongue, which may explain why we observe intermittency at a relatively large detuning. It is worth noting that our full experimental campaign covers a wide range of forcing frequencies ($f_f/f_n \in [0.30, 2.10]$), enabling synchronisation to be detected in the 2:1, 1:1 and 1:2 Arnold tongues. Between the 1:1 and 1:2 tongues, we find the classic Ruelle–Takens–Newhouse route to chaos, along which the dressed winding number (f_n^*/f_f) approaches the golden mean ($\sigma_g = (\sqrt{5}-1)/2$) and the distribution of spectral peaks aligns with the Fibonacci sequence. Thus, for certain forcing conditions at the onset of chaos, the jet obeys the universal scaling properties of the sine circle map (Olinger & Sreenivasan 1988; Ott 2002). We also find the period-doubling route to chaos around the 2:1 tongue, as well as strange non-chaotic attractors and crisis-induced intermittency around the 1:2 tongue. Currently, we are conducting a detailed analysis of these different transition scenarios to better understand the complex jet dynamics. This complexity underscores the importance of exercising caution when selecting the forcing parameters for the open-loop control of globally unstable jets.

Acknowledgements. We would like to thank Yuanhang Zhu, Vikrant Gupta and Kelvin Leung for fruitful discussions.

Funding. This work was funded by the Research Grants Council of Hong Kong (project nos. 16210419 and 16200220).

Declaration of interests. The authors report no conflict of interest.

Author ORCIDs.
Bo Yin https://orcid.org/0000-0002-4323-7150;
Yu Guan https://orcid.org/0000-0003-4454-3333;
Larry K.B. Li https://orcid.org/0000-0002-0820-170X.

References

Afraimovich, V.S. & Shilnikov, L.P. 1991 Invariant two-dimensional tori, their breakdown and stochasticity. *Am. Math. Soc. Transl* **149** (2), 201–212.

Arneodo, A., Coullet, P. & Tresser, C. 1981 Possible new strange attractors with spiral structure. *Commun. Math. Phys.* **79**, 573–579.

Aronson, D.G., Chory, M.A., Hall, G.R. & McGehee, R.P. 1982 Bifurcations from an invariant circle for two-parameter families of maps of the plane: a computer-assisted study. *Commun. Math. Phys.* **83**, 303–354.

Boccaletti, S., Grebogi, C., Lai, Y.C., Mancini, H. & Maza, D. 2000 The control of chaos: theory and applications. *Phys. Rep.* **329** (3), 103–197.

Bonetti, M. & Boon, J.P. 1989 Chaotic dynamics in open flow: the excited jet. *Phys. Rev.* A **40** (6), 3322.

Broze, G. & Hussain, F. 1996 Transitions to chaos in a forced jet: intermittency, tangent bifurcations and hysteresis. *J. Fluid Mech.* **311**, 37–71.

Chakravarthy, R.V.K., Lesshafft, L. & Huerre, P. 2018 Global stability of buoyant jets and plumes. *J. Fluid Mech.* **835**, 654–673.

Chomaz, J.M., Huerre, P. & Redekopp, L.G. 1988 Bifurcations to local and global modes in spatially developing flows. *Phys. Rev. Lett.* **60** (1), 25.

Coenen, W., Lesshafft, L., Garnaud, X. & Sevilla, A. 2017 Global instability of low-density jets. *J. Fluid Mech.* **820**, 187–207.

Danaila, I., Dušek, J. & Anselmet, F. 1998 Nonlinear dynamics at a Hopf bifurcation with axisymmetry breaking in a jet. *Phys. Rev.* E **57** (4), R3695.

Feigenbaum, M.J. 1978 Quantitative universality for a class of nonlinear transformations. *J. Stat. Phys.* **19** (1), 25–52.

Fraser, A.M. & Swinney, H.L. 1986 Independent coordinates for strange attractors from mutual information. *Phys. Rev.* A **33** (2), 1134–1140.

Ganapathy, R. & Sood, A.K. 2006 Intermittency route to rheochaos in wormlike micelles with flow-concentration coupling. *Phys. Rev. Lett.* **96** (10), 108301.

Gollub, J.P. & Benson, S.V. 1980 Many routes to turbulent convection. *J. Fluid Mech.* **100** (3), 449–470.

Gottwald, G.A. & Melbourne, I. 2004 A new test for chaos in deterministic systems. *Proc. R. Soc. Lond.* A **460** (2042), 603–611.

Grassberger, P. & Procaccia, I. 1983 Characterization of strange attractors. *Phys. Rev. Lett.* **50** (5), 4.

Griffith, T.M., Parthimos, D., Crombie, J. & Edwards, D.H. 1997 Critical scaling and type-III intermittent chaos in isolated rabbit resistance arteries. *Phys. Rev.* E **56** (6), 6287.

Hallberg, M.P. & Strykowski, P.J. 2006 On the universality of global modes in low-density axisymmetric jets. *J. Fluid Mech.* **569**, 493–507.

Huerre, P. & Monkewitz, P.A. 1990 Local and global instabilities in spatially developing flows. *Annu. Rev. Fluid Mech.* **22**, 473–537.

Kushwaha, A.K., Worth, N.A., Dawson, J.R., Gupta, V. & Li, L.K.B. 2022 Asynchronous and synchronous quenching of a globally unstable jet via axisymmetry breaking. *J. Fluid Mech.* **937**, A40.

Kyle, D.M. & Sreenivasan, K.R. 1993 The instability and breakdown of a round variable-density jet. *J. Fluid Mech.* **249**, 619–664.

Lee, M., Zhu, Y., Li, L.K.B. & Gupta, V. 2019 System identification of a low-density jet via its noise-induced dynamics. *J. Fluid Mech.* **862**, 200–215.

Lesshafft, L. & Marquet, O. 2010 Optimal velocity and density profiles for the onset of absolute instability in jets. *J. Fluid Mech.* **662**, 398–408.

Li, L.K.B. & Juniper, M.P. 2013*a* Lock-in and quasiperiodicity in a forced hydrodynamically self-excited jet. *J. Fluid Mech.* **726**, 624–655.

Li, L.K.B. & Juniper, M.P. 2013*b* Phase trapping and slipping in a forced hydrodynamically self-excited jet. *J. Fluid Mech.* **735** (R5), 1–11.

Manneville, P. 2010 *Instabilities, Chaos and Turbulence*, 2nd edn. Imperial College Press.

Monkewitz, P.A., Bechert, D.W., Barsikow, B. & Lehmann, B. 1990 Self-excited oscillations and mixing in a heated round jet. *J. Fluid Mech.* **213**, 611–639.

Nair, A.B., Deohans, A. & Vinoth, B.R. 2022 Global oscillations in low-density round jets with parabolic velocity profiles. *J. Fluid Mech.* **941**, A44.

Newhouse, S., Ruelle, D. & Takens, F. 1978 Occurrence of strange Axiom A attractors near quasiperiodic flows on $\mathbb{T}^m$, $m \geqq 3$. *Commun. Math. Phys.* **64** (1), 35–40.

Nuñez, A., Lacasa, L., Valero, E., Gómez, J.P. & Luque, B. 2012 Detecting series periodicity with horizontal visibility graphs. *Intl J. Bifurcation Chaos* **22** (07), 1250160.

OLINGER, D.J. & SREENIVASAN, K.R. 1988 Nonlinear dynamics of the wake of an oscillating cylinder. *Phys. Rev. Lett.* **60** (9), 797–800.

OTT, E. 2002 *Chaos in Dynamical Systems*, 2nd edn. Cambridge University Press.

PASCHE, S., AVELLAN, F. & GALLAIRE, F. 2018 Onset of chaos in helical vortex breakdown at low Reynolds number. *Phys. Rev. Fluids* **3** (6), 064701.

PIKOVSKY, A., ROSENBLUM, M. & KURTHS, J. 2003 *Synchronization: A Universal Concept in Nonlinear Sciences*. Cambridge University Press.

POMEAU, Y. & MANNEVILLE, P. 1980 Intermittent transition to turbulence in dissipative dynamical systems. *Commun. Math. Phys.* **74** (2), 189–197.

SACHER, J., ELSÄSSER, W. & GÖBEL, E.O. 1989 Intermittency in the coherence collapse of a semiconductor laser with external feedback. *Phys. Rev. Lett.* **63** (20), 2224–2227.

SCHMID, P.J. & HENNINGSON, D.S. 2001 *Stability and Transition in Shear Flows*. Springer.

SCHUSTER, H.G. & JUST, W. 2005 *Deterministic Chaos*, 4th edn. Wiley.

SREENIVASAN, K.R., RAGHU, S. & KYLE, D. 1989 Absolute instability in variable density round jets. *Exp. Fluids* **7** (5), 309–317.

SUJITH, R.I. & UNNI, V.R. 2020 Complex system approach to investigate and mitigate thermoacoustic instability in turbulent combustors. *Phys. Fluids* **32** (6), 061401.

TAKENS, F. 1981 Detecting strange attractors in turbulence. In *Dynamical Systems and Turbulence* (ed. D. Rand & L.S. Young), vol. 898, pp. 366–381. Springer Berlin Heidelberg.

ZHU, Y., GUPTA, V. & LI, L.K.B. 2017 Onset of global instability in low-density jets. *J. Fluid Mech.* **828**, R1.

ZHU, Y., GUPTA, V. & LI, L.K.B. 2019 Coherence resonance in low-density jets. *J. Fluid Mech.* **881**, R1.